Engineering 5 (2019) 287–295

Contents lists available at ScienceDirect

Engineering

journal homepage: www.elsevier.com/locate/eng

Research
Synthetic Biology—Article

Engineering the Biosynthesis of Caffeic Acid in *Saccharomyces cerevisiae* with Heterologous Enzyme Combinations

Lanqing Liu [a,b,#], Hong Liu [a,b,#], Wei Zhang [a,b], Mingdong Yao [a,b], Bingzhi Li [a,b], Duo Liu [a,b,*], Yingjin Yuan [a,b]

[a] *Key Laboratory of Systems Bioengineering (Ministry of Education), School of Chemical Engineering and Technology, Tianjin University, Tianjin 300072, China*
[b] *SynBio Research Platform, Collaborative Innovation Center of Chemical Science and Engineering (Tianjin), Tianjin University, Tianjin 300072, China*

ARTICLE INFO

Article history:
Received 21 March 2018
Revised 25 September 2018
Accepted 20 November 2018
Available online 02 March 2019

Keywords:
Saccharomyces cerevisiae
Caffeic acid
Heterologous enzyme
Cytochrome P450
Synthetic biology

ABSTRACT

Engineering the biosynthesis of plant-derived natural products in microbes presents several challenges, especially when the expression and activation of the plant cytochrome P450 enzyme is required. By recruiting two enzymes—HpaB and HpaC—from several bacteria, we constructed functional 4-hydroxyphenylacetate 3-hydroxylase (4HPA3H) in *Saccharomyces cerevisiae* to take on a role similar to that of the plant-derived cytochrome P450 enzyme and produce caffeic acid. Along with a common tyrosine ammonia lyase (TAL), the different combinations of HpaB and HpaC presented varied capabilities in producing the target product, caffeic acid, from the substrate, *L*-tyrosine. The highest production of caffeic acid was obtained with the enzyme combination of HpaB from *Pseudomonas aeruginosa* and HpaC from *Salmonella enterica*, which yielded up to (289.4 ± 4.6) $mg \cdot L^{-1}$ in shake-flask cultivation. The compatibility of heterologous enzymes within a yeast chassis was effectively improved, as the caffeic acid production was increased by 40 times from the initial yield. Six key amino acid residues around the flavin adenine dinucleotide (FAD) binding domain in HpaB from *Pseudomonas aeruginosa* were differentiate from those other HpaBs, and might play critical roles in affecting enzyme activity. We have thus established an effective approach to construct a highly efficient yeast system to synthesize non-native hydroxylated phenylpropanoids.

1. Introduction

A typical characteristic of synthetic biology is the recruitment of enzymes from different species in order to charge multi-step biochemical reactions to synthesize functional products. One of the most famous examples of this process involved utilizing enzymes from plants, mammals, bacteria, and yeast itself to construct a plant's opioid biosynthetic pathway in *Saccharomyces cerevisiae* (*S. cerevisiae*), which consisted of more than 20-step reactions [1]. The model microbes *Escherichia coli* (*E. coli*) and *S. cerevisiae* have also been engineered to optimally synthesize other plant-derived natural products such as artemisinic acid, paclitaxel precursors, salvianic acid A, and ginsenoside [2–8]. The choice of heterologous enzymes was carefully considered in order to achieve desirable product synthesis efficiency. A particularly daunting—but not impossible—task when rebuilding a plant-derived hydroxylation reaction in microbes is to screen and modify a functional cytochrome P450 enzyme from heterologous resources. Plant cytochrome P450 usually needs to be anchored on the special membrane structures of organelles such as mitochondria and the endoplasmic reticulum, and requires the assistance of co-enzymes such as NADPH and $FADH_2$. This highly specialized working mode restricts the enzyme activity of cytochrome P450 in engineered microbes [9,10].

The valuable product caffeic acid is synthesized in plants through reactions in which cytochromes P450 participate. This natural product, also known as 3,4-dihydroxycinnamic acid, along with its derivatives, such as chlorogenic acid (CGA) and caffeic acid phenethyl ester (CAPE), is broadly used in medicine, food, and other life-health applications [11–14]. The content of caffeic acid in natural plants is quite low, and the current un-matured extraction method further decreases its productivity and purity [15]. Thus, using a synthetic biology method to construct a microbe to produce caffeic acid is seen as a promising choice [16]. A direct

* Corresponding author.
E-mail address: liuduo19870401@126.com (D. Liu).
# These authors contributed equally.

https://doi.org/10.1016/j.eng.2018.11.029

route would be to recruit the plant-derived deamination reaction of phenylalanine—a two-step hydroxylation at the 4- and 3-positions of the benzyl ring—to obtain cinnamic acid and *p*-coumaric acid [17,18]. The involved enzymes are cinnamate 4-hydroxylase (C4H) and *p*-coumarate 3-hydroxylase (Coum3H), which are plant-specific cytochrome P450-dependent monooxygenases [19,20]. However, only a few reports have shown that plant-derived C4H functions in microbes, and no successful examples of such functioning of plant-derived Coum3H have been reported [21,22]. A quite different way would be to engineer biosynthetic pathway in *E. coli*. Lin and Yan [9] determined that the *E. coli*-native 4-hydroxyphenlacetate 3-hydroxylase (4HPA3H) can successfully hydroxylate the substrate *p*-coumaric acid to caffeic acid. Rodrigues et al. [10] used cytochrome P450 CYP199A2 from *Rhodopseudomonas palustris* to convert *p*-coumaric acid to caffeic acid. Zhang and Stephanopoulos [23] used 4-coumarate: coenzyme A ligase (4CL) and Coum3H encoded by *sam5* from *Saccharothrix espanaensis* to synthesize caffeic acid from coumaric acid. They also examined the TAL and Coum3H pathway for synthesizing caffeic acid from tyrosine. Yao from our research group constructed a heterogeneous salvianic acid A pathway from the substrate 4-hydroxyphenylpyruvate, using 4-hydroxyphenylacetate 3-monooxygenase (HpaB) and NADPH-flavin oxidoreductase (HpaC) cloned from *E. coli* [24]. The catalysis activity of HpaB and HpaC on a broad substrate scope has been proven [9,24]. These works paved the way for the engineering biosynthesis of caffeic acid in microbes independent of plant-derived cytochrome P450 enzymes [25,26] (Fig. 1(a)).

In the present work, we successfully constructed a caffeic acid biosynthetic pathway in *S. cerevisiae* by employing a heterologous tyrosine ammonia lyase (TAL) and a 4HPA3H complex composed of HpaB and HpaC derived from different species (Fig. 1(b)). The *hpaB* and *hpaC* genes were *de novo* synthesized after codon optimization for expression in *S. cerevisiae*. By co-transforming three plasmids, including the transcriptional unit (TU) of one common *TAL* and respective combinations of *hpaB* and *hpaC* TUs, we constructed several yeast strains that produced caffeic acid. This method facilitated a rapid test of the abilities of different enzyme combinations for caffeic acid production. The results showed that the combination of *hpaB* from *Pseudomonas aeruginosa* (*P. aeruginosa*) and *hpaC* from *Salmonella enterica* yielded the highest level of caffeic acid, at (289.4 ± 4.6) $mg{\cdot}L^{-1}$ in shake-flask fermentation. The optimal combination of HpaB and HpaC showed compatibility with the yeast chassis, which is promising for the highly efficient production of caffeic acid and other valuable derivatives.

2. Materials and methods

2.1. Heterologous genes synthesis and construction of plasmids

Table 1 lists the plasmids used in this study. The gene sequence of *Rhodosporidium toruloides* (*R. toruloides*) TAL was downloaded from the National Center of Biotechnology Information (NCBI) database[†] and was delivered to GenScript Biotech Corp. for *de novo* synthesis after codon optimization. The corresponding gene sequences of HpaB and HpaC, derived from several species, were also obtained from the NCBI database and synthesized in the same way. These genes were localized on pUC57-Simple-01 to 15 vectors, respectively, where a natural *Bsa*I site in pUC57 was mutated.

The promoters P_{PDC1}, P_{PGK1}, and P_{TDH3} and the terminators T_{ENO2}, T_{GPM1}, T_{GPD}, T_{CYC1}, and T_{TEF1} were cloned by polymerase chain reaction (PCR) from the genome of yeast strain BY4741. Then T_{ENO2}, P_{PDC1}, and T_{GPM1} were assembled in order by overlap extension polymerase chain reaction (OE-PCR) with designed special primers to form a new cassette, T_{ENO2}–P_{PDC1}–T_{GPM1}, which was a model of the blank TU used in our work [27]. We designed two back-to-back *BsaI* enzyme recognizing and cutting sites between P_{PDC1} and T_{GPM1} to prepare for the subsequent digestion (Fig. 1(b)). In parallel, T_{GPM1}–P_{PGK1}–T_{GPD} and T_{CYC1}–P_{TDH3}–T_{TEF1} were also respectively constructed. All these cassettes were digested with *NotI* and ligated separately into the different plasmids pRS415, pRS413, and pRS416, generating pRS415-Blank, pRS413-Blank, and pRS416-Blank.

The gene segments of *hpaB*, *hpaC*, and *TAL* were digested with *BsaI* and recovered from their respective pUC57-Simple plasmids; they were then ligated into individual pRS415-Blank, pRS413-Blank, and pRS413-Blank for the construction of TUs. All the constructed TUs are listed in Table 1 as pRS415-hpaB-01 to -07, pRS413–hpaC-01 to -07, and pRS416-TAL, where -01 to -05 refer to the amino acid sequences of *hapB* and/or *hapC* from sources of *E. coli*, *Klebsiella pneumoniae*, *Photorhabdus luminescens*, *P. aeruginosa*, and *P. putida* respectively, hapB-06 and -07 refer to the source of *Sulfobacillus acidophilus TPY* and *E. cloacae,* and *hapC*-06 and -07 refer to the source of *Salmonella enterica* and *Achromobacter* sp. In addition, the genes *Coum3H* and *CYP199A2* were ligated into pRS415-Blank, forming pRS415-Coum3H and pRS415-CYP199A2.

2.2. Co-transformation of plasmids

The *E. coli* TransT1 competence cells used for plasmid cloning were cultured in Luria-Bertani medium supplemented at 37 °C with 100 $\mu g{\cdot}mL^{-1}$ of kanamycin or 100 $\mu g{\cdot}mL^{-1}$ of ampicillin for selection. The constructed plasmids (Table 1) with the backbones of pRS416, pRS415, and pRS413 were selected according to the design (Section 3). They were co-transformed into *S. cerevisiae* strain BY4741 by means of the LiAc/PEG method and cultured on a nutrition-deficient petri dish [28,29]. Table 2 lists the strains that were used in this study. Synthetic complete (SC) medium lacking uracil, leucine, and histidine (SC-Ura-Leu-His) was used to select the right transformants, except for SyBE_Sc03020101 and SyBE_Sc03020102, which were grown in SC-Ura-Leu medium. All the strains were cultivated overnight at 30 °C and 250 $r{\cdot}min^{-1}$. We then transferred the pre-culture liquid into 20 mL of fresh medium under the same conditions until the mid-log growing phase. After about 20 h, the seed culture was inoculated into 50 mL of SC medium with an initial OD_{600} (optical density measured at a wavelength of 600 nm) of 0.2 and cultivated at 30 °C and 250 $r{\cdot}min^{-1}$ for 96 h under aerobic fermentation using 12 layer sterile gauze to close the flask. In all cases, an extra 0.5 $g{\cdot}L^{-1}$ of *L*-tyrosine was added to the medium at the beginning. All the fermentation experiments were performed in triplicate.

2.3. Extraction and quantification of caffeic acid and p-coumaric acid

After fermentation, the yeast cells were collected and centrifuged. An equal volume of ethyl acetate was added to the supernatant medium and the cell pellets, respectively; next, both mixtures were vortexed drastically to extract the caffeic acid and *p*-coumaric acid. This step was performed twice. The organic phase was collected in a new tube and dried with nitrogen flow, and then the residue was dissolved in methanol as the extracted product samples. The extracts were analyzed on a Alliance® high-performance liquid chromatography (HPLC) system with a separation module e2695 and a 2487 detector (Waters Corporation, USA). The chromatographic software used was MassLynx V4.0. An Ascentis® Express C18 column (10 cm × 2.1 mm, 2.7 μm particle size, Sigma-Aldrich Corporation, USA) was used. The mobile phase comprised solvent A (methanol) and C (water containing 0.1% (v/v) formic acid); the gradient eluted program used is listed in Table 3. The

[†] https://www.ncbi.nlm.nih.gov.

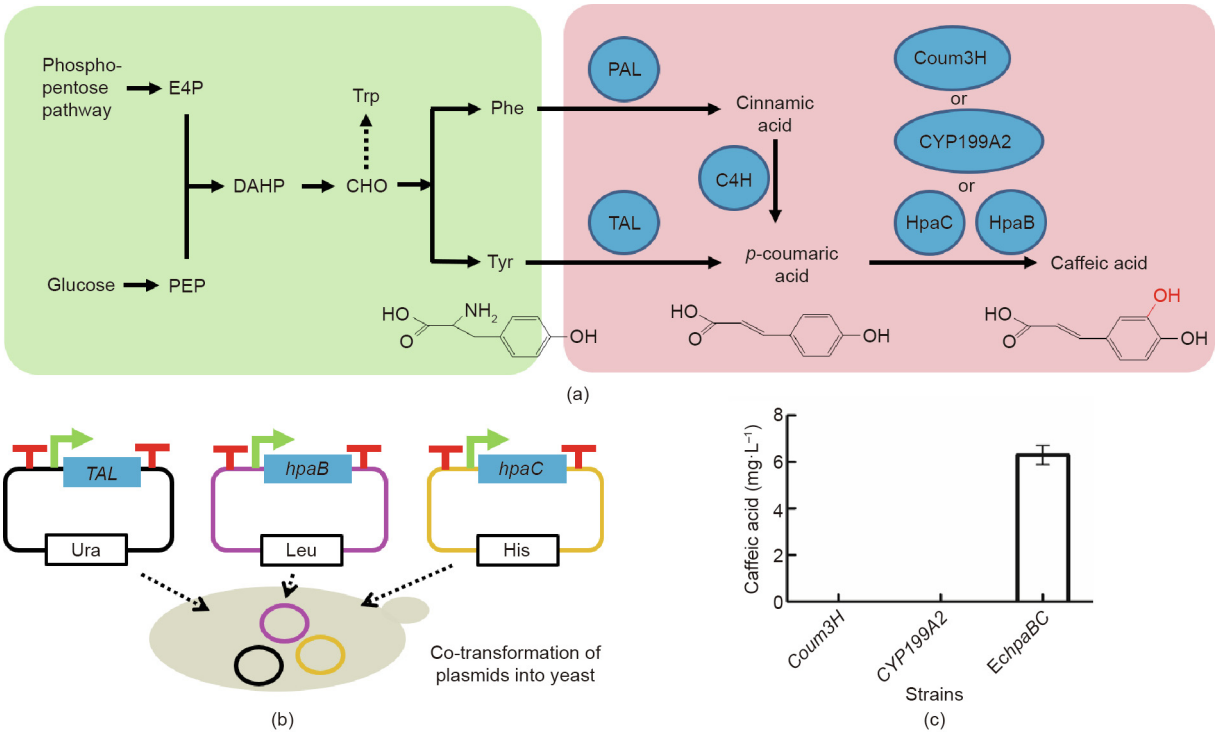

Fig. 1. Construction of pathways of caffeic acid biosynthesis in *S. cerevisiae*. (a) The paradigm of the caffeic acid biosynthetic pathway that had been successfully constructed in engineered *E. coli*; (b) schematic plot of *in vivo* co-transformation of multiple plasmids utilized to test the constructed pathway in yeast; (c) detected caffeic acid production in yeast containing different pathways. E4P: erythrose-4-phosphate; PEP: phosphoenolpyruvate; DAHP: 3-deoxy-*D*-arabinoheptulosonate-7-phosphate; CHO: chorismic acid; Phe: phenylalanine; Trp: Tryptophan; Tyr: tyrosine; Ura: uracil; Leu: Leucine; His: Histidine.

flow rate was 0.2 mL·min^{-1}, the column temperature was 35 °C, and the injection volume was 5 μL. The wavelength for detecting caffeic acid was 326 nm and the wavelength for detecting *p*-coumaric acid was 310 nm. The products were confirmed by the retention time, compared with those of authentic standards.

2.4. Bioinformatic analysis and structural simulation of hpaB

The amino acid sequences of *hpaB* from seven sources—*E. coli* (Ec*hpaB*), *Klebsiella pneumoniae* (Kp*hpaB*), *Photorhabdus luminescens* (Pl*hpaB*), *P. aeruginosa* (Pa*hpaB*), *P. putida* (Pp*hpaB*), *Sulfobacillus acidophilus TPY* (Sa*hpaB*), and *E. cloacae* (En*hpaB*)—were aligned by ClustalW2[†] with default settings. The crystal structure of HpaB with the ligand flavin adenine dinucleotide (FAD) was stimulated according to a *Thermus thermophilus HB8* with a similar structure (PDB ID: 2YYL, Protein Data Bank, USA) by the webserver SWISS-MODEL[‡]. Based on the homologous structure, a binding domain in HpaB was determined/predicted [30,31].

3. Results and discussion

3.1. Primary construction of caffeic acid biosynthetic pathway in yeast

A first challenge of utilizing cytochrome P450 was to synthesize *p*-coumaric acid from phenylalanine by means of the action of C4H. Since tyrosine also possesses a 4-hydroxyl group, it can also be directly converted to *p*-coumaric acid by a TAL (Fig. 1(a)). Based on our previous work, a TAL from *R. toruloides* was demonstrated to be fully functional in the biosynthesis of resveratrol and naringenin in *S. cerevisiae* [32,33]. Therefore, we used this TAL to synthesize *p*-coumaric acid from *L*-tyrosine and obtained a yield of 117.5 mg·L^{-1}, which was equivalent with that of other works [33].

The next challenge was to synthesize caffeic acid from *p*-coumaric acid using cytochrome P450 Coum3H. As previously stated, the idea of converting *p*-coumaric acid to caffeic acid in *E. coli* has been shown to be viable using various other enzymes as well as using Coum3H [9]. In order to test the availability of these enzymes as heterogenous enzymes in *S. cerevisiae* (Fig. 1), we applied different TUs on plasmids and co-transformed the plasmids into yeast (see Section 2, Tables 1 and 2). As shown in Fig. 1 (c), neither the codon-optimized *Coum3H* from *Rhodopseudomonas palustris* nor *CYP199A2* from *Saccharothrix espanaensis* worked in yeast, as no caffeic acid production was detected. To test the function of *hpaB* and *hpaC* derived from *E. coli*, we designed three options for the transformation of yeast cells: only the TU of T_{ENO2}-P_{PDC1}-Ec*hpaB*-T_{GPM1} on pRS415; only the TU of T_{GPM1}-P_{PGK1}-Ec*hpaC*-T_{GPD} on pRS413; and both plasmids. In each case, a partner T_{CYC1}-P_{TDH3}-*TAL*-T_{TEF1} on pRS416 was also transformed. As a result, only the pathway containing *TAL* and both *hpaB* and *hpaC* resulted in a small peak of caffeic acid, as detected by HPLC. This initial production of caffeic acid in yeast was slight, at (6.3 ± 0.3) mg·L^{-1} (Appendix A. Fig. S1). The necessity of both HpaB and HpaC for synthesizing the target product in yeast was thus primarily verified.

The finding that the single enzymes of *Coum3H* and *CYP199A2*, respectively, did not function, while the combination of HpaB and HpaC did function in yeast indicated the potential importance of heterologous enzyme combinations. A single heterologous enzyme contains multiple domains and may not have good compatibility with yeast. By contrast, HpaB and HpaC might have the advantage of labor division—an idea that was tested later. It was supposed that other species-derived HpaBC combinations might work better than the enzymes from *E. coli*, as they might show

[†] http://www.ebi.ac.uk/Tools/msa/clustalw2.
[‡] https://swissmodel.expasy.org.

Table 1
Plasmids used in this study.

Plasmid	Description	Source
pRS415	Single copy plasmid with *LEU2* and *ampR* marker	—
pRS413	Single copy plasmid with *HIS3* and *ampR* marker	—
pRS416	Single copy plasmid with *URA3* and *ampR* marker	—
pUC57-Simple	Blunt cloning vector, *kanR* marker	GenScript
pUC57-Simple-01	*hpaB* from *E. coli* (protein accession No.: AAR11357.1)	GenScript
pUC57-Simple-02	*hpaB* from *Klebsiella pneumoniae* (CDO16163.1)	GenScript
pUC57-Simple-03	*hpaB* from *Photorhabdus luminescens* (AAO17197.1)	GenScript
pUC57-Simple-04	*hpaB* from *P. aeruginosa* (PKG21040.1)	GenScript
pUC57-Simple-05	*hpaB* from *P. putida* (ADA63516.1)	GenScript
pUC57-Simple-06	*hpaB* from *Sulfobacillus acidophilus* TPY (AEJ40622.1)	GenScript
pUC57-Simple-07	*hpaB* from *Enterobacter cloacae* (PJG38870.1)	GenScript
pUC57-Simple-08	*hpaC* from *E. coli* (AAR11356.1)	GenScript
pUC57-Simple-09	*hpaC* from *Klebsiella pneumoniae* (CDO16164.1)	GenScript
pUC57-Simple-10	*hpaC* from *Photorhabdus luminescens* (AAO17198.1)	GenScript
pUC57-Simple-11	*hpaC* from *P. aeruginosa* (PKG21041.1)	GenScript
pUC57-Simple-12	*hpaC* from *P. putida* (ADA63517.1)	GenScript
pUC57-Simple-13	*hpaC* from *Salmonella enterica* (GAR62209.1)	GenScript
pUC57-Simple-14	*hpaC* from *Achromobacter* sp. (CUJ32851.1)	GenScript
pUC57-Simple-15	*TAL* from *R. toruloides* (CDR39392.1)	GenScript
pUC57-Simple-101	*Coum3H* from *Saccharothrix espanaensis* (ABC88666.1)	GenScript
pUC57-Simple-102	*CYP199A2* from *Rhodopseudomonas palustris* (OPF94131.1)	GenScript
pRS415-Blank	The cassette T_{ENO2}-P_{PDC1}-(back-to-back *BsaI* sites)-T_{GPM1} was cloned and inserted into the *NotI* site of pRS415	This study
pRS413-Blank	The cassette T_{GPM1}-P_{PGK1}-(back-to-back *BsaI* sites)-T_{GPD} was cloned and inserted into the *NotI* site of pRS413	This study
pRS416-Blank	The cassette T_{CYC1}-P_{TDH3}-(back-to-back *BsaI* sites)-T_{TEF1} was cloned and inserted into the *NotI* site of pRS416	This study
pRS415-hpaB-01, 02, 03, 04, 05, 06, 07	*hpaB* was digested from pUC57-Simple-01, 02, 03, 04, 05, 06, 07 by *BsaI* and inserted between the digested back-to-back *BsaI* sites in pRS415-Blank	This study
pRS413-hpaC-01, 02, 03, 04, 05, 06, 07	*hpaC* was digested from pUC57-Simple-08, 09, 10, 11, 12, 13, 14 by *BsaI* and inserted between the digested back-to-back *BsaI* sites in pRS413-Blank	This study
pRS416-TAL	*TAL* was digested from pUC57-Simple-15 by *BsaI* and inserted between the digested back-to-back *BsaI* sites in pRS416-Blank	This study
pRS415-Coum3H	*Coum3H* was ligated into pRS415-Blank	This study
pRS415-CYP199A2	*CYP199A2* was ligated into pRS415-Blank	This study

Table 2
S. cerevisiae strains used in this study.

Strain	Description: chassis strain (plasmids contained)
BY4741	*MATa; his3Δ1; leu2Δ0; met15Δ0; ura3Δ0*
SyBE_Sc03020001	BY4741 (pRS416-TAL, pRS415-Blank and pRS413-Blank)
SyBE_Sc03020002	BY4741 (pRS416-TAL, pRS415-hpaB-01, pRS413-hpaC-01)
SyBE_Sc03020003	BY4741 (pRS416-TAL, pRS415-hpaB-02, pRS413-hpaC-02)
SyBE_Sc03020004	BY4741 (pRS416-TAL, pRS415-hpaB-03, pRS413-hpaC-03)
SyBE_Sc03020005	BY4741 (pRS416-TAL, pRS415-hpaB-04, pRS413-hpaC-04)
SyBE_Sc03020006	BY4741 (pRS416-TAL, pRS415-hpaB-05, pRS413-hpaC-05)
SyBE_Sc03020007	BY4741 (pRS416-TAL, pRS415-hpaB-01, pRS413-hpaC-04)
SyBE_Sc03020008	BY4741 (pRS416-TAL, pRS415-hpaB-02, pRS413-hpaC-04)
SyBE_Sc03020009	BY4741 (pRS416-TAL, pRS415-hpaB-03, pRS413-hpaC-04)
SyBE_Sc03020010	BY4741 (pRS416-TAL, pRS415-hpaB-05, pRS413-hpaC-04)
SyBE_Sc03020011	BY4741 (pRS416-TAL, pRS415-hpaB-06, pRS413-hpaC-04)
SyBE_Sc03020012	BY4741 (pRS416-TAL, pRS415-hpaB-07, pRS413-hpaC-04)
SyBE_Sc03020013	BY4741 (pRS416-TAL, pRS415-hpaB-04, pRS413-hpaC-01)
SyBE_Sc03020014	BY4741 (pRS416-TAL, pRS415-hpaB-04, pRS413-hpaC-02)
SyBE_Sc03020015	BY4741 (pRS416-TAL, pRS415-hpaB-04, pRS413-hpaC-03)
SyBE_Sc03020016	BY4741 (pRS416-TAL, pRS415-hpaB-04, pRS413-hpaC-05)
SyBE_Sc03020017	BY4741 (pRS416-TAL, pRS415-hpaB-04, pRS413-hpaC-06)
SyBE_Sc03020018	BY4741 (pRS416-TAL, pRS415-hpaB-04, pRS413-hpaC-07)
SyBE_Sc03020019	BY4741 (pRS416-TAL, pRS415-hpaB-01, pRS413-hpaC-06)
SyBE_Sc03020020	BY4741 (pRS416-TAL, pRS415-hpaB-02, pRS413-hpaC-06)
SyBE_Sc03020021	BY4741 (pRS416-TAL, pRS415-hpaB-03, pRS413-hpaC-06)
SyBE_Sc03020022	BY4741 (pRS416-TAL, pRS415-hpaB-05, pRS413-hpaC-06)
SyBE_Sc03020023	BY4741 (pRS416-TAL, pRS415-hpaB-06, pRS413-hpaC-06)
SyBE_Sc03020024	BY4741 (pRS416-TAL, pRS415-hpaB-07, pRS413-hpaC-06)
SyBE_Sc03020101	BY4741 (pRS416-TAL, pRS415-Coum3H)
SyBE_Sc03020102	BY4741 (pRS416-TAL, pRS415-CYP199A2)

All strains were sourced by this study.

better compatibility with the yeast chassis. Furthermore, the key co-enzyme NADPH or $FADH_2$ might take on an essential role in the activity of HpaB and HpaC [25,26]. These aspects were considered and tested as follows.

3.2. Testing other hpaB and hpaC from the same species for caffeic acid production

Although the functions of HpaB and HpaC had been primarily verified, the efficiency of synthesizing caffeic acid was far from satisfactory. It was speculated that other natural alternatives from other species might work better. Therefore, we searched for other, possibly better, enzyme performers. A key point was how to set a standard in order to select options. We searched for counterparts of *E. coli*-derived *hpaB* and *hpaC*, respectively, using the Position-Specific Iterative Basic Local Alignment Search Tool (PSI-BLAST), and found that no more than 10 resources shared a relatively high similarity with *E. coli* counterparts (> 90%). More than 10 resources shared a similarity of between 80% and 90%, while nearly 20 resources shared a similarity of 70%–80% with *E. coli* counterparts. In general, the similarity of *hpaB* was slightly higher than that of *hpaC* from the same species resource. With full consideration of both the species distance and the enzyme sequence similarity, we chose four species for gene selection: *Klebsiella pneumoniae* (Kp*hpaB*, similarity: 96%; Kp*hpaC*, similarity: 85%), *Photorhabdus luminescens* (Pl*hpaB*, similarity: 82%; Pl*hpaC*, similarity: 77%), *P. aeruginosa* (Pa*hpaB*, similarity: 73%; Pa*hpaC*, similarity: 58%), and *P. putida* (Pp*hpaB*, similarity: 42%; Pp*hpaC*, similarity: 25%). All of these sources belong to gram-negative bacilli. All the genes were *de novo* synthesized according to protein sequences after codon optimization.

Relevant plasmids were constructed using the same approach and co-transformed into yeast to obtain the target strains (Tables 1 and 2). Strains were cultured under the same fermentation conditions. Fig. 2 shows the detected yields of caffeic acid and *p*-coumaric acid. The strains SyBE_Sc03020003 (Kp*hpaB*, Kp*hpaC*) and SyBE_Sc03020004 (Pl*hpaB*, Pl*hpaC*) resulted in even less caffeic acid production than SyBE_Sc03020002 (Ec*hpaB*, Ec*hpaC*), with the *p*-coumaric acid only slightly being transformed to caffeic acid (as 1.2 and 2.1 $mg{\cdot}L^{-1}$, respectively). The situation improved significantly in the strain SyBE_Sc03020005 (Pa*hpaB*, Pa*hpaC*), with an improvement of caffeic acid production to 68.2 $mg{\cdot}L^{-1}$ an increase in nearly 11-fold from production with SyBE_Sc03020002. Amazingly, more than half of the precursor *p*-coumaric acid was successfully transformed, and only 35.96 $mg{\cdot}L^{-1}$ of *p*-coumaric acid was left. In the strain SyBE_Sc03020006 (Pp*hpaB*, Pp*hpaC*), although the expressed enzymes shared a low similarity with *E. coli* enzymes, the caffeic acid production was significant: 1.7-fold higher, at 16.8 $mg{\cdot}L^{-1}$. To sum up, different species-derived enzyme couples showed distinguishable compatibility with the

Table 3
HPLC gradient eluted conditions for caffeic acid and *p*-coumaric acid.

Time (min)	Mobile phase proportion (%)				Flow rate (mL·min^{-1})	Curve
	A	B	C	D		
0	15	0	85	0	0.2	1
2.00	35	0	65	0	0.2	6
5.00	55	0	45	0	0.2	6
8.00	55	0	45	0	0.2	6
8.50	15	0	85	0	0.2	1
15.00	15	0	85	0	0.2	6

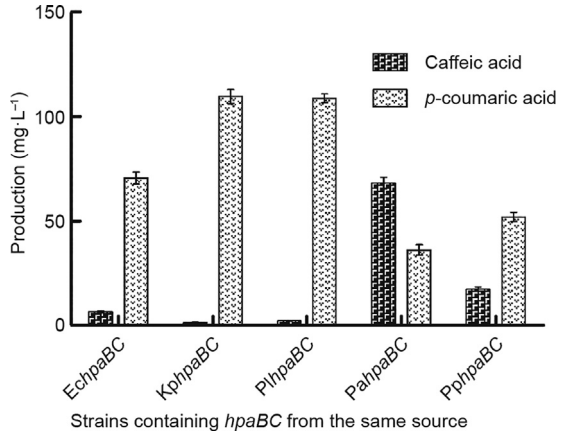

Fig. 2. Production of caffeic acid and its precursor *p*-coumaric acid in different strains containing combinations of *hpaB* and *hpaC* from common sources. The error bars represent standard deviations calculated from triplicate experiments in shake-flask fermentation.

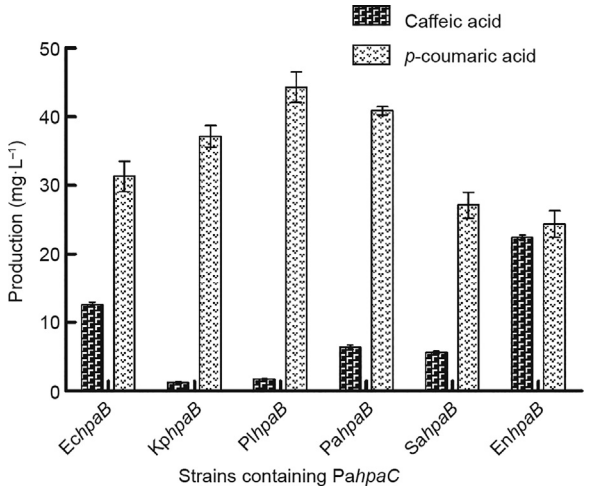

Fig. 3. The effect of Pa*hpaC* combined with other *hpaB*s on caffeic acid production. Strains containing the same Pa*hpaC* and diverse *hpaB* showed variable yields of caffeic acid and *p*-coumaric acid. The error bars represent standard deviations calculated from triplicate experiments in shake-flask fermentation.

yeast chassis. We considered that the roles of Pa*hpaB* and Pa*hpaC*, contained in the strain SyBE_Sc03020005, was worthy of further studies.

3.3. The effect of Pa hpaC combined with other hpaBs on caffeic acid production

Since the HpaB and HpaC from *P. aeruginosa* were optimally selected for fairly good caffeic acid production, we considered testing whether one of the two enzymes could collaborate even better with other species-derived enzymes. The combinatorial screening of enzymes from diverse sources has been shown to be a promising way to determine the best combination for higher productivity of the target main compound in terms of substrate selectivity, catalytic activity, and host cell compatibility [34–36]. Pa*hpaC* was chosen first for a study of its collaboration with other species-derived *hpaB*, since the HpaC enzyme acts first to synthesize the co-enzyme $FADH_2$ from NADPH, and then transfers the $FADH_2$ to the HpaB enzyme for the hydroxylation reaction [26]. Relevant plasmids were constructed earlier and selectively co-transformed into yeast cells for further fermentation under the same conditions (Fig. 3, Tables 1 and 2). The highest detected caffeic acid production was 12.8 mg·L^{-1} with SyBE_Sc03020007 (Ec*hpaB*, Pa*hpaC*), which was still much lower than the 68.7 mg·L^{-1} obtained with SyBE_Sc03020005 (Pa*hpaB*, Pa*hpaC*). Other combinations resulted in minimal caffeic acid production, ranging from 1.3 to 6.8 mg·L^{-1}. These results indicated that HpaC might not be the bottleneck enzyme.

In order to further verify this speculation, we employed other two *hpaB* genes derived from Sa*hpaB* and *E. cloacae* (En*hpaB*) in combination with Pa*hpaC*. The former combination caused the strain to produce 5.7 mg·L^{-1}of caffeic acid, and the latter combination resulted in 22.7 mg·L^{-1} of caffeic acid—still not comparative with the higher production that had been obtained with SyBE_Sc03020005 (Pa*hpaB*, Pa*hpaC*). It was also seen that more than half of the *p*-coumaric acid was already transformed in most strains (Fig. 3). The largest amount of remaining *p*-coumaric acid occurred with SyBE_Sc03020009 (Pl*hpaB*, Pa*hpaC*), at 44.2 mg·L^{-1}, and the least remaining *p*-coumaric acid occurred with SyBE_Sc03020012 (En*hpaB*, Pa*hpaC*), at 24.9 mg·L^{-1}. However, the precursor was not delivered thoroughly to produce caffeic acid. Thus, a potential intermediate state might exist between the actions of HpaC and HpaB. Overall, HpaC was primarily shown not to charge the bottleneck step of the reaction.

3.4. The effect of Pa hpaB combined with other hpaCs on caffeic acid production

Next, Pa*hpaB* was chosen for a study of its collaboration with other species-derived *hpaC*. Previous reports have indicated that *hpaB* might play the key role in the catalysis reaction from *p*-coumaric acid to caffeic acid [25,37,38]. To test this finding, the already-used *hpaC* genes were first combined with Pa*hpaB*. Relevant plasmids were constructed and co-transformed into yeast, and the fermentation followed (Fig. 4(a), Tables 1 and 2). The experimental results showed, astonishingly, that the PaHpaB enzyme worked well with other HpaC enzymes in yeast—in fact, much better than their natural couples. The caffeic acid production with SyBE_Sc03020013 (Pa*hpaB*, Ec*hpaC*) was 37.6 mg·L^{-1}.

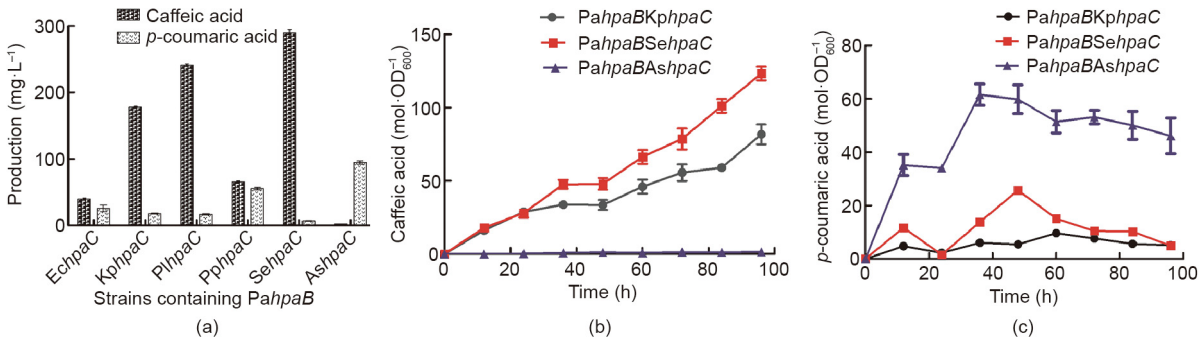

Fig. 4. The effect of Pa*hpaB* combined with other *hpaC*s on caffeic acid production. (a) Strains containing the same Pa*hpaB* and diverse *hpaC* showed variable yields of caffeic acid and *p*-coumaric acid. The error bars represent standard deviations calculated from triplicate experiments in shake-flask fermentation. (b) The yields of caffeic acid and (c) *p*-coumaric acid during the time course. The error bars represent standard deviation calculated from triplicate experiments.

The production with SyBE_Sc03020016 (Pa*hpaB*, Pp*hpaC*) was 68.49 mg·L^{-1}—nearly the same as that in the previous optimal strain, SyBE_Sc03020005 (Pa*hpaB*, Pa*hpaC*). With SyBE_Sc03020014 (Pa*hpaB*, Kp*hpaC*) and SyBE_Sc03020015 (Pa*hpaB*, Pl*hpaC*), the caffeic acid yields were 175.86 and 241.3 mg·L^{-1}, respectively, and 80% of the *p*-coumaric acid had been transformed, leaving only 17.8 and 16.8 mg·L^{-1}, respectively. The HPLC trace of caffeic acid and *p*-coumaric acid are documented in the Appendix A (Fig. S1). The Kp*hpaC* and Pl*hpaC* offered higher compatibility with Pa*hpaB* in yeast cells than the natural partner, Pa*hpaC*.

In order to seek an even more efficient coupling of the two enzymes, we chose two other new *hpaC* genes from *Salmonella enterica* (Se*hpaC*) and *Achromobacter* sp. (As*hpaC*), respectively, to collaborate with Pa*hpaB*. Up to this point, the maximum yield of caffeic acid had been obtained in strain SyBE_Sc03020017 containing Pa*hpaB* and Se*hpaC*, at (289.4 ± 4.6) mg·L^{-1} (Fig. 4(a), Fig. S1). The products of SyBE_Sc03020017 were also characterized using time-of-flight mass spectrometry (TOF-MS) and time-of-flight mass spectrometry/mass spectrometry (TOF-MS/MS) (liquid chromatography was performed using the ACQUITY UHPLC system (Waters Corporation, USA) and a Xevo G2-S Q-Tof mass spectrometer equipped with an electrospray ionization (ESI) ion source was used (Waters Corporation, USA)) in Fig. S2. The characterized negative ions (107, 117, 135, 146, 161, 174, and 179) were identical with those in the mass spectrum of caffeic acid. This yield was almost 240 times greater than the minimum yield in strain SyBE_Sc03020003 and nearly 43 times greater than the yield in the initial tested strain, SyBE_Sc03020002 with Ec*hpaB* and Ec*hpaC*. In SyBE_Sc03020017, more than 90% of the *p*-coumaric acid was transferred and only 6.9 mg·L^{-1} was left. This extremely low remaining amount of *p*-coumaric acid and high yield of caffeic acid indicated that the reactions under the control of the SeHpaC and PaHpaB enzymes probably pulled more flux through *L*-tyrosine synthesis from the endogenous metabolism. Another HpaC, from As*hpaC*, did not collaborate well with Pa*hpaB* and resulted in a caffeic acid production of only 2.7 mg·L^{-1}.

The cell density, caffeic acid accumulation, and decrease in *p*-coumaric acid in the strains SyBE_Sc03020015, SyBE_Sc03020017, and SyBE_Sc03020018 were measured during the time course (Fig. 4(b) and (c)). SyBE_Sc03020017 (Pa*hpaB*, Se*hpaC*) produced caffeic acid at the highest level, at (124.4 ± 2.4) mol·OD_{600}^{-1}. For most of the fermentation period, the production of *p*-coumaric acid was lower than 20 mol·OD_{600}^{-1}. In addition, the production of caffeic acid maintained an increasing tendency when at 96 h. This finding further verified our speculation that the highly efficient cooperation of HpaB and HpaC could pull more carbon resources from the endogenous metabolism. Overall, HpaB primarily charged the potential bottleneck step, but still required an appropriate HpaC partner to achieve high efficiency of the whole reaction.

3.5. The effect of SehpaC combined with other hpaBs on caffeic acid production

As the combination of SeHpaC and PaHpaB appeared to be the champion strain, we speculated that this newly constructed TU of HpaC might also collaborate well with other HpaB. To test this, the plasmid containing the TU of Se*hpaC* was co-transformed with other already-used *hpaB* TU-plasmids, respectively, into yeast, as well as the TAL-containing plasmid (Fig. 5, Tables 1 and 2). The results showed that this Se*hpaC* did not cooperate well with *hpaB* other than Pa*hpaB*. In strain SyBE_Sc03020013 (Pa*hpaB*, Ec*hpaC*), the caffeic acid yield was relatively higher, at 23.2 mg·L^{-1}. In the other strains, less than 10 mg·L^{-1}of caffeic acid was synthesized. In the strains of SyBE_Sc03020019 (Ec*hpaB*, Se*hpaC*), SyBE_Sc03020020 (Kp*hpaB*, Se*hpaC*), and SyBE_Sc03020021 (Pl*hpaB*, Se*hpaC*), SeHpaC turned out to be almost inactive, as most of the precursor *p*-coumaric acid remained unreacted. In the strains of SyBE_Sc03020022 (Pp*hpaB*, Se*hpaC*), SyBE_Sc03020023 (Sa*hpaB*, Se*hpaC*), and SyBE_Sc03020024 (En*hpaB*, Se*hpaC*), SeHpaC turned out to be active enough to transfer *p*-coumaric acid, although the yield of the final product, caffeic acid, was still low. Based on our data, this result implied that HpaC and HpaB impact each other, probably through the transfer of the co-enzyme $FADH_2$. This co-enzyme, which is synthesized from NADPH by HpaC, is highly unstable and easily breaks down if it is not utilized in time by the next HpaB enzyme. In conclusion, it was found to be important to analyze why special enzyme combinations worked much

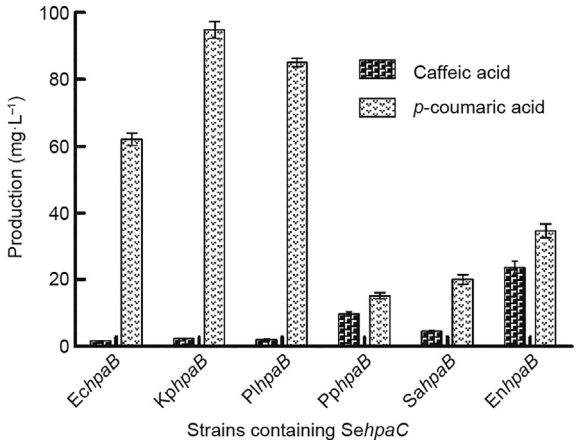

Fig. 5. The effect of Se*hpaC* combined with other *hpaB*s on caffeic acid production. Strains containing the same Se*hpaC* and diverse *hpaB* showed variable yields of caffeic acid and *p*-coumaric acid. The error bars represent standard deviations calculated from triplicate experiments in shake-flask fermentation.

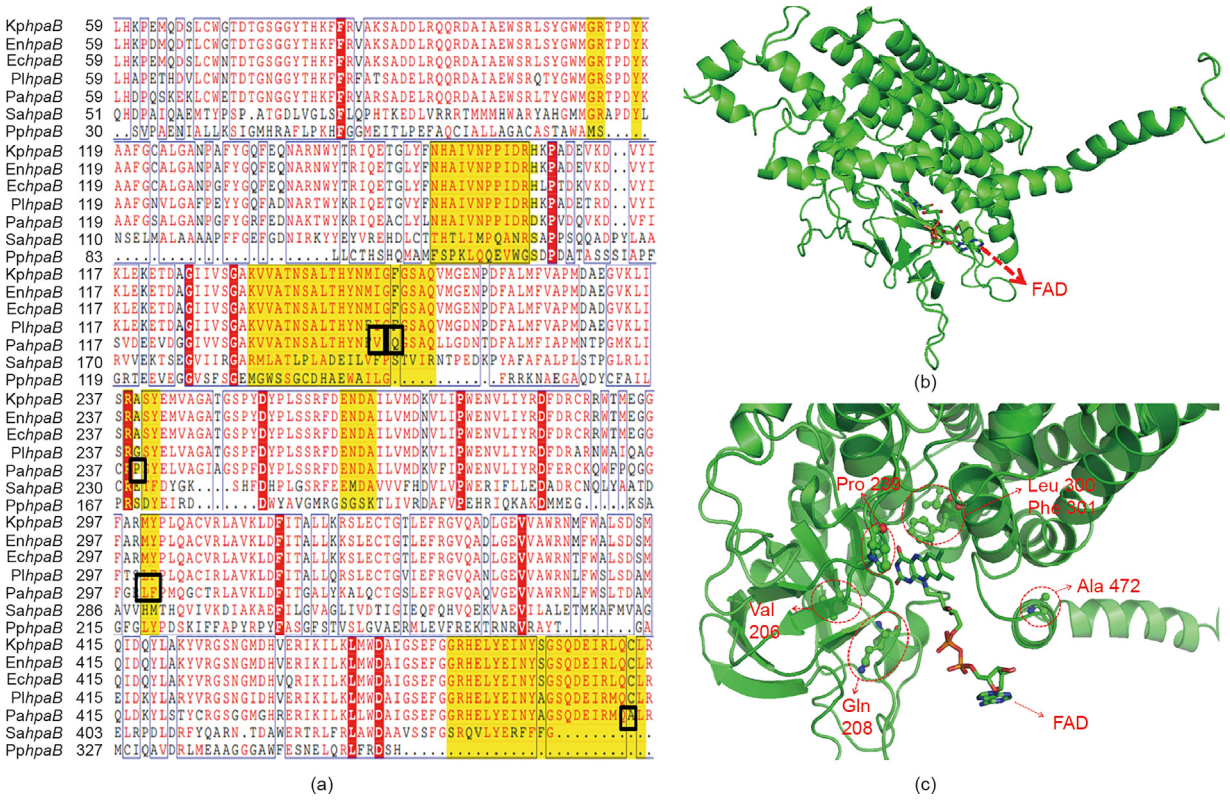

Fig. 6. Sequence differences among diverse *hpaB* sources and structural simulation of the *hpaB* from *P. aeruginosa*. (a) Amino acid sequences alignment of *hpaB* from seven sources. (b) Structural simulation of HpaB in the best combination, according to the crystal structure of *Thermus thermophilus* HB8 with the ligand FAD. (c) The putative amino acid active binding sites are circled and denoted in red. Val: valine; Gln: glutamine; Pro: proline; Ala: alanine.

better, and even overwhelmed other combinations. The co-enzyme transfer between HpaB and HpaC might be a key point.

3.6. Protein structure analysis of the key enzyme HpaB

All of our data and analysis were consistent with what had been reported previously: that is, that HpaB might play the key role in the conversion process from *p*-coumaric acid to caffeic acid [25,38]. The study of the enzyme's catalytic active binding sites with the co-enzyme substrate became meaningful in progressively improving the caffeic acid production. In addition to strongly focusing on the HpaB from *P. aeruginosa*, all the amino acid sequences of already-used HpaB (i.e., Ec*hpaB*, Kp*hpaB*, Pl*hpaB*, Pa*hpaB*, Pp*hpaB*, Sa*hpaB*, and En*hpaB*) were aligned using ClustalW2 with default settings [39]. According to the alignment results shown in Fig. 6(a), some distinct amino acids were found among the key binding sites; these were recorded and are marked with yellow boxes in the figure. The yellow boxes were determined according to the following process: First, we obtained the available crystal structure of *hpaB* from *Thermus thermophilus* HB8 with the ligand FAD [9]. Next, the crystal structures of the *hpaB* proteins used in our work were constructed by homologous protein simulation with SWISS-MODEL using *hpaB* from *Thermus thermophilus* HB8 as the template, as shown in Fig. 6(b). The sequence identity between *hpaB* from *P. aeruginosa* and the template ranged from 45% to 53%. This homologous simulation process allowed us to predict the approximate binding domains between *hpaB* and its substrate, which were finally labeled yellow in Fig. 6(a). We recorded these amino acid sites at the same time, given all the information described above.

It was reasonable to predict that the amino acids with yellow boxes had strong connections with catalytic reaction activity, according to our structural simulation. Since the sequences of SaHpaB and PpHpaB in yellow boxes shared quite low homology with those of other HpaBs, it was not meaningful to consider them when exploring the key binding sites. Only the differences between the champion PaHpaB and the other four highly homologous HpaBs were considered. Finally, six important amino acid residues—valine 206, glutamine 208, proline 239, leucine 300, phenylalanine 301, and alanine 472—were identified as the potential key sites, since they were uniquely present in the champion PaHpaB (Fig. 6(c)). As shown in the figure, these residues were located all around the FAD binding domain. It was speculated that these six residues had key impacts on the catalytic bioactivity of HpaB. Of course, these putative essential sites still require verification via point mutagenesis in further studies. To sum up, we generally exploited the potential reason why the *hpaB* from *P. aeruginosa* showed the highest activity in order to provide a new research possibility to improve the yield of caffeic acid.

4. Conclusion

Synthetic biology has realized the biosynthesis of plant-derived natural compounds in engineered microbial chassis via the construction of heterologous pathways [40]. The direct implantation of plant-derived genes in microbes is sometimes—but not always—possible. One strategy involves using an exact substitution of the plant enzymes. For example, in the engineered biosynthesis of caffeic acid in microbes, two nearest substitutions of the plant cytochrome P450 enzyme—Coum3H and CYP199A2—were derived from *Saccharothrix espanaensis* and *Rhodopseudomonas palustris*, respectively, and successfully used in engineered *E. coli* in previous works [10,21,41,42]. In our study, a more robust model microbial chassis, *S. cerevisiae*, was engineered to achieve caffeic acid

production. Coum3H and CYP199A2 were tested first, but showed no detectable function in yeast for the synthesis of caffeic acid. By contrast, the co-introduction of HpaB and HpaC, which collaborate as a whole in the form of 4HPA3H, was found to be successful in yeast for caffeic acid synthesis, with an initial caffeic acid production of (6.3 ± 0.3) mg·L^{-1}. The respective works of Lin and Yao have also shown that these enzymes are functional in *E. coli* [9,24].

Even though the initial designed pathways containing the enzymes of TAL and EcHpaB and EcHpaC functioned, the efficiency of converting the substrate into the end product was insufficient. The catalytic activity of the enzymes encoded by genes of different species often varies greatly; thus, optimizing the combination of individual genes screened from several different species is an effective way to improve the efficiency of heterologous reactions [34,43]. Here, we selectively synthesized and constructed *hpaB* and *hpaC* from several bacterial resources to obtain new combinations of 4HPA3H. The results showed that the productions of caffeic acid in all strains were quite distinguishable. The combinations containing Pa*hpa*B (*hpaB* from *P. aeruginosa*) all showed acceptable and relatively high production of caffeic acid. Through combinatorial manipulation of *hpaB* and *hpaC* enzymes, the caffeic acid yield was significantly improved by 45.9-fold (from 6.3 to 289.4 mg·L^{-1}) in shake flask fermentation in the optimal strain SyBE_Sc03020017, as compared with the starting strain SyBE_Sc03020002 that contained both *hpaB* and *hpaC* from *E. coli*. It was also primarily shown that the appropriate cooperation of both HpaB and HpaC was extremely important for driving more flux toward the product synthesis from the endogenous metabolic resources.

Furthermore, in order to explore the root cause why some gene combinations generated higher production of caffeic acid, we analyzed the activities of the key gene *hpaB* by simulation. We located six active amino acid sites that may play necessary roles in catalysis—valine 206, glutamine 208, proline 239, leucine 300, phenylalanine 301, and alanine 472—all of which are located around the FAD binding domain. We consider that the FAD-binding action determines the activity of *hpaB* and the final combination of *hpaB* and *hpaC*. This speculation reveals a possible future direction for modifying the enzyme's activities. To sum up, we have successfully created the biosynthesis of caffeic acid in yeast for the first time, and achieved a maximum yield of (289.4 ± 4.6) mg·L^{-1}; this yield is one of the best yields of caffeic acid in engineered microbes. Our study provides a promising insight into key enzyme manipulation in collaborative reactions for the microbial overproduction of desired phenol compounds.

Acknowledgements

This work was funded by the Ministry of Science and Technology of China (2014CB745100) and the National Natural Science Foundation of China (21390203 and 21706186).

Compliance with ethics guidelines

Lanqing Liu, Hong Liu, Wei Zhang, Mingdong Yao, Bingzhi Li, Duo Liu, and Yingjin Yuan declare that they have no conflict of interest or financial conflicts to disclose.

Appendix A. Supplementary data

Supplementary data to this article can be found online at https://doi.org/10.1016/j.eng.2018.11.029.

References

[1] Galanie S, Thodey K, Trenchard IJ, Filsinger Interrante M, Smolke CD. Complete biosynthesis of opioids in yeast. Science 2015;349(6252):1095–100.
[2] Martin VJ, Pitera DJ, Withers ST, Newman JD, Keasling JD. Engineering a mevalonate pathway in *Escherichia coli* for production of terpenoids. Nat Biotechnol 2003;21(7):796–802.
[3] Ro DK, Paradise EM, Ouellet M, Fisher KJ, Newman KL, Ndungu JM, et al. Production of the antimalarial drug precursor artemisinic acid in engineered yeast. Nature 2006;440(7086):940–3.
[4] Paddon CJ, Westfall PJ, Pitera DJ, Benjamin K, Fisher K, McPhee D, et al. High-level semi-synthetic production of the potent antimalarial artemisinin. Nature 2013;496(7446):528–32.
[5] Ajikumar PK, Xiao WH, Tyo KE, Wang Y, Simeon F, Leonard E, et al. Isoprenoid pathway optimization for Taxol precursor overproduction in *Escherichia coli*. Science 2010;330(6000):70–4.
[6] Zhou K, Qiao K, Edgar S, Stephanopoulos G. Distributing a metabolic pathway among a microbial consortium enhances production of natural products. Nat Biotechnol 2015;33(4):377–83.
[7] Nakagawa A, Matsumura E, Koyanagi T, Katayama T, Kawano N, Yoshimatsu K, et al. Total biosynthesis of opiates by stepwise fermentation using engineered *Escherichia coli*. Nat Commun 2016;7(1):10390.
[8] Liu D, Li B, Liu H, Li BZ, Yuan YJ. Profiling influences of gene overexpression on heterologous resveratrol production in *Saccharomyces cerevisiae*. Front Chem Sci Eng 2017;11(1):1–9.
[9] Lin Y, Yan Y. Biosynthesis of caffeic acid in *Escherichia coli* using its endogenous hydroxylase complex. Microb Cell Fact 2012;11(1):42.
[10] Rodrigues JL, Araújo RG, Prather KL, Kluskens LD, Rodrigues LR. Heterologous production of caffeic acid from tyrosine in *Escherichia coli*. Enzyme Microb Technol 2015;71:36–44.
[11] Yoshimoto M, Kurata-Azuma R, Fujii M, Hou DX, Ikeda K, Yoshidome T, et al. Enzymatic production of caffeic acid by koji from plant resources containing caffeoylquinic acid derivatives. Biosci Biotechnol Biochem 2005;69(9):1777–81.
[12] Sachan A, Ghosh S, Sen SK, Mitra A. Co-production of caffeic acid and *p*-hydroxybenzoic acid from *p*-coumaric acid by *Streptomyces caeruleus* MTCC 6638. Appl Microbiol Biotechnol 2006;71(5):720–7.
[13] De Campos Buzzi F, Franzoi CL, Antonini G, Fracasso M, Cechinel Filho V, Yunes RA, et al. Antinociceptive properties of caffeic acid derivatives in mice. Eur J Med Chem 2009;44(11):4596–602.
[14] Wu J, Omene C, Karkoszka J, Bosland M, Eckard J, Klein CB, et al. Caffeic acid phenethyl ester (CAPE), derived from a honeybee product propolis, exhibits a diversity of anti-tumor effects in pre-clinical models of human breast cancer. Cancer Lett 2011;308(1):43–53.
[15] Xing Y, Peng HY, Zhang MX, Li X, Zeng WW, Yang XE. Caffeic acid product from the highly copper-tolerant plant *Elsholtzia splendens* post-phytoremediation: its extraction, purification, and identification. J Zhejiang Univ Sci B 2012;13(6):487–93.
[16] Celik S, Erdogan S, Tuzcu M. Caffeic acid phenethyl ester (CAPE) exhibits significant potential as an antidiabetic and liver-protective agent in streptozotocin-induced diabetic rats. Pharmacol Res 2009;60(4):270–6.
[17] Bourgaud F, Hehn A, Larbat R, Doerper S, Gontier E, Kellner S, et al. Biosynthesis of coumarins in plants: a major pathway still to be unravelled for cytochrome P450 enzymes. Phytochem Rev 2006;5(2–3):293–308.
[18] Nakamura S, Minami A, Fujimoto K, Kojima T. Combination effect of recombinant human interleukin-1 alpha with antimicrobial agents. Antimicrob Agents Chemother 1989;33(10):1804–10.
[19] Cheniany M, Ganjeali A. Developmental role of phenylalanine-ammonia-lyase (PAL) and cinnamate 4-hydroxylase (C4H) genes during adventitious rooting of *Juglans regia* L. microshoots. Acta Biol Hung 2016;67(4):379–92.
[20] Kim YH, Kwon T, Yang HJ, Kim W, Youn H, Lee JY, et al. Gene engineering, purification, crystallization and preliminary X-ray diffraction of cytochrome P450 *p*-coumarate-3-hydroxylase (C3H), the *Arabidopsis* membrane protein. Protein Expr Purif 2011;79(1):149–55.
[21] Ro DK, Mah N, Ellis BE, Douglas CJ. Functional characterization and subcellular localization of poplar (*Populus trichocarpa* × *Populus deltoides*) cinnamate 4-hydroxylase. Plant Physiol 2001;126(1):317–29.
[22] Li M, Schneider K, Kristensen M, Borodina I, Nielsen J. Engineering yeast for high-level production of stilbenoid antioxidants. Sci Rep 2016;6(1):36827.
[23] Zhang H, Stephanopoulos G. Engineering *E. coli* for caffeic acid biosynthesis from renewable sugars. Appl Microbiol Biotechnol 2013;97(8):3333–41.
[24] Yao YF, Wang CS, Qiao J, Zhao GR. Metabolic engineering of *Escherichia coli* for production of salvianic acid A via an artificial biosynthetic pathway. Metab Eng 2013;19:79–87.
[25] Huang Q, Lin Y, Yan Y. Caffeic acid production enhancement by engineering a phenylalanine over-producing *Escherichia coli* strain. Biotechnol Bioeng 2013;110(12):3188–96.
[26] Prieto MA, Garcia JL. Molecular characterization of 4-hydroxyphenylacetate 3-hydroxylase of *Escherichia coli*. A two-protein component enzyme. J Biol Chem 1994;269(36):22823–9.
[27] Heckman KL, Pease LR. Gene splicing and mutagenesis by PCR-driven overlap extension. Nat Protoc 2007;2(4):924–32.
[28] Gietz RD, Woods RA. Yeast transformation by the LiAc/SS carrier DNA/PEG method. Methods Mol Biol 2006;313:107–20.

[29] Nell RE, Phillips RH. Contributions of brewers' yeast to a diet deficient in reproductive factors. J Nutr 1950;42(1):117–27.
[30] Liu Z, Fu J, Shan L, Sun Q, Zhang W. Synthesis, preliminary bioevaluation and computational analysis of caffeic acid analogues. Int J Mol Sci 2014;15(5):8808–20.
[31] Xiao P, Zhang S, Ma H, Zhang A, Lv X, Zheng L. Stereoselective synthesis of caffeic acid amides via enzyme-catalyzed asymmetric aminolysis reaction. J Biotechnol 2013;168(4):552–9.
[32] Zhang W, Liu H, Li X, Liu D, Dong XT, Li FF, et al. Production of naringenin from *D*-xylose with co-culture of *E. coli* and *S. cerevisiae*. Eng. Life Sci 2017;17(9):1021–9.
[33] Rodriguez A, Kildegaard KR, Li M, Borodina I, Nielsen J. Establishment of a yeast platform strain for production of *p*-coumaric acid through metabolic engineering of aromatic amino acid biosynthesis. Metab Eng 2015;31:181–8.
[34] Kim E, Moore BS, Yoon YJ. Reinvigorating natural product combinatorial biosynthesis with synthetic biology. Nat Chem Biol 2015;11(9):649–59.
[35] Sarria S, Wong B, García Martín H, Keasling JD, Peralta-Yahya P. Microbial synthesis of pinene. ACS Synth Biol 2014;3(7):466–75.
[36] Zhao S, Jones JA, Lachance DM, Bhan N, Khalidi O, Venkataraman S, et al. Improvement of catechin production in *Escherichia coli* through combinatorial metabolic engineering. Metab Eng 2015;28:43–53.
[37] Xun L, Sandvik ER. Characterization of 4-hydroxyphenylacetate 3-hydroxylase (HpaB) of *Escherichia coli* as a reduced flavin adenine dinucleotide-utilizing monooxygenase. Appl Environ Microbiol 2000;66(2):481–6.
[38] Galán B, Díaz E, Prieto MA, García JL. Functional analysis of the small component of the 4-hydroxyphenylacetate 3-monooxygenase of *Escherichia coli* W: a prototype of a new flavin:NAD(P)H reductase subfamily. J Bacteriol 2000;182(3):627–36.
[39] Larkin MA, Blackshields G, Brown NP, Chenna R, McGettigan PA, McWilliam H, et al. Clustal W and Clustal X version 2.0. Bioinformatics 2007;23(21):2947–8.
[40] Luo Y, Li BZ, Liu D, Zhang L, Chen Y, Jia B, et al. Engineered biosynthesis of natural products in heterologous hosts. Chem Soc Rev 2015;44(15):5265–90.
[41] Choi O, Wu CZ, Kang SY, Ahn JS, Uhm TB, Hong YS. Biosynthesis of plant-specific phenylpropanoids by construction of an artificial biosynthetic pathway in *Escherichia coli*. J Ind Microbiol Biotechnol 2011;38(10):1657–65.
[42] Kang SY, Choi O, Lee JK, Hwang BY, Uhm TB, Hong YS. Artificial biosynthesis of phenylpropanoic acids in a tyrosine overproducing *Escherichia coli* strain. Microb Cell Fact 2012;11(1):153.
[43] Chai F, Wang Y, Mei X, Yao M, Chen Y, Liu H, et al. Heterologous biosynthesis and manipulation of crocetin in *Saccharomyces cerevisiae*. Microb Cell Fact 2017;16(1):54.